Physical properties of rare-earth metal-ion vermiculite intercalation compounds

Itsuko S. Suzuki, Jaime Morrilo, Charles R. Burr, and Masatsugu Suzuki
Department of Physics, State University of New York at Binghamton, Binghamton, New York 13902-6000
(Received 3 September 1993; revised manuscript received 2 February 1994)

The structural and magnetic properties of vermiculite intercalation compounds (VIC's) with two-water-layer hydration states having Ce^{3+}, Pr^{3+}, Nd^{3+}, Sm^{3+}, Eu^{3+}, Gd^{3+}, Tb^{3+}, Dy^{3+}, Ho^{3+}, and Er^{3+} ions in the interlamellar space between the host silicate layers have been studied by means of ($00L$) x-ray scattering, dc magnetic susceptibility, and thermogravimetric measurements. The intercalate layer sandwiched between two water layers consists of u cations and w water molecules per unit rectangular cell of $(a \times b)$: $u = 0.5-0.69, w = 0-4.0$. The c-axis repeat distance is found to be roughly proportional to the ionic radius, giving indirect evidence for the strong rigidity of the host silicate layers. The magnetic susceptibility of these compounds shows a Curie-Weiss behavior. The Curie-Weiss temperature Θ for Ce^{3+}, Pr^{3+}, Nd^{3+}, and Sm^{3+} is described by $\Theta = -1.58J(J+1)$ [K], while Θ for Gd^{3+}, Tb^{3+}, Dy^{3+}, Ho^{3+}, and Er^{3+} is described by $\Theta = 0.93(g_J-1)^2J(J+1)$ [K]. The Eu^{3+} VIC shows a Van Vleck susceptibility in the temperature range between 50 and 300 K.

I. INTRODUCTION

The vermiculite intercalation compounds (VIC's) are well-characterized expanding layered silicates, where each host silicate layer is composed of two tetrahedral sheets coupled symmetrically to an octahedral sheet.[1] In order to balance the charge deficiency due to isomorphic substitution of Al^{3+} for Si^{4+} in tetrahedral sheets, the cations are introduced into the interlamellar space between host silicate layers. Naturally occurring vermiculite has Mg^{2+} ions as cations and is denoted by the Mg^{2+} VIC. The Llano vermiculite used for the present experiment has the unit-cell stoichiometry[2]

$$(Si_{5.72}Al_{2.28})(Mg_{5.88}Al_{0.10}Fe_{0.03}Ti_{0.02})$$
$$O_{20}(OH)_4Mg_{0.93}(H_2O)_w \ .$$

The Mg^{2+} ions in the interlamellar space between the host silicate layers can be easily exchanged by various kinds of magnetic ions such as transition-metal ions (Mn^{2+}, Co^{2+}, Ni^{2+}, Cu^{2+}) and rare-earth metal ions (Ce^{3+}, Pr^{3+}, Nd^{3+}, Sm^{3+}, Eu^{3+}, Gd^{3+}, Tb^{3+}, Dy^{3+}, Ho^{3+}, Er^{3+}), forming magnetic VIC's. The magnetic VIC's have three kinds of hydration states defined by the number of water layers in the interlamellar space; zero-, one-, and two-water-layer hydration states (WLHS).[3] In the 1-WLHS the water molecules normally lie in the same plane as the cations. In the 2-WLHS, the magnetic cations are usually sandwiched between upper and lower water layers. The hydration state depends on the water vapor pressure and temperature. The magnetic VIC's are frequently in the 2-WLHS under normal ambient conditions. The c-axis repeat distance d is typically given by $d \approx 14.4$ Å for transition-metal-ion VIC's with 2-WLHS and $d \approx 14.9$ Å for rare-earth metal-ion VIC's with 2-WLHS.[4] Because of the large c-axis repeat distance, the magnetic VIC's may provide the model system for studying two-dimensional (2D) magnetism.

There have been several studies[5-8] on the magnetic properties of magnetic VIC's such as the Mn^{2+}, Co^{2+}, Ni^{2+}, Cu^{2+}, Dy^{3+}, and Er^{3+} VIC's by dc magnetic susceptibility measurements. Suzuki *et al.*[5] have measured the dc magnetic susceptibility of Mn^{2+}, Co^{2+}, Ni^{2+}, Cu^{2+}, Dy^{3+}, and Er^{3+} VIC's with 2-WLHS. These magnetic VIC's show no magnetic phase transition in the temperature range between 4.2 and 300 K. The dc magnetic susceptiblity of these compounds obeys the Curie-Weiss law. The Curie-Weiss temperature Θ of Ni^{2+}, Dy^{3+}, and Er^{3+} VIC's with 2-WLHS is positive, indicating that the intraplanar exchange interaction between like ions is ferromagnetic. The Curie-Weiss temperature of Mn^{2+}, Co^{2+}, and Cu^{2+} VIC's with 2-WLHS is close to zero but negative. The unit-cell stoichiometry of magnetic VIC's with 2-WLHS has been determined from dc magnetic susceptibility and thermogravimetric measurement.[5] The number of cations in the unit cell was determined as $u = 0.76 \pm 0.08$ for Mn^{2+}, Co^{2+}, and Ni^{2+} VIC's, $u = 1.12 \pm 0.07$ for Cu^{2+} VIC, $u = 0.59$ for Dy^{3+} VIC, and $u = 0.60$ for Er^{3+} VIC, respectively. The in-plane structure of the host silicate layer is distorted from a regular honeycomb, and has a rectangular unit cell of $(a \times b)$ with the lattice constants $a = 5.34$ and $b = 9.30$ Å.[1] The rare-earth metal ions are considered to form a triangular lattice with the nearest-neighbor (NN) distance 9.24 Å, which is close to the $u = \frac{2}{3}$ type $(3a \times b)$ commensurate structure where there are two rare-earth metal ions per $(3a \times b)$ unit cell. Nishihara *et al.*[6] have shown that the high-field magnetization in the Ni^{2+} VIC with 2-WLHS is well described by the model of the quasi-2D magnetic system with predominant ferromagnetic intraplanar exchange interaction and weak antiferromagnetic interplanar exchange interaction. Wada *et al.*[7] have reported a preliminary result on ac magnetic susceptibility of the Ni^{2+} VIC with 2-WLHS, indicating some evidence for magnetic phase transitions at 2.3 and 3.4 K. Recently Zhou *et al.*[8] have reported the results of dc magnetic susceptibility for Mn^{2+}, Co^{2+}, Ni^{2+}, and Cu^{2+} VIC's having 0- and 2-WLHS in the temperature range between 2

and 300 K. They have shown that the Co^{2+} and Ni^{2+} VIC's with 0-WLHS undergo antiferromagnetic phase transitions at 5 and 3 K, respectively. The Co^{2+} and Ni^{2+} VIC's with 2-WLHS are paramagnetic and obey the Curie-Weiss law. The Mn^{2+} and Cu^{2+} VIC's are paramagnetic for temperatures down to 2 K regardless of the hydration state.

In this paper we have undertaken extensive studies on the structural and magnetic properties of rare-earth metal ion VIC's such as Ce^{3+}, Pr^{3+}, Nd^{3+}, Sm^{3+}, Eu^{3+}, Gd^{3+}, Tb^{3+}, Dy^{3+}, Ho^{3+}, and Er^{3+} VIC's with 2-WLHS. As far as we know, this is the first systematic investigation of rare-earth metal-ion VIC's. We determine the c-axis repeat distance of these compounds from $(00L)$ x-ray scattering, and discuss the relationship between the c-axis repeat distance and ionic radius. In order to explain the $(00L)$ x-ray-scattering intensities, we propose a model of the c-axis stacking sequence for rare-earth metal VIC's with 2-WLHS, which is different from that for transition-metal-ion VIC's. We report experimental results on the dc magnetic susceptibility of these compounds. The dc magnetic susceptibility obeys a Curie-Weiss law. The Eu^{3+} and Sm^{3+} VIC's require the Van Vleck susceptibility for the explanation of these magnetic properties. We show that the Curie-Weiss temperature of Gd^{3+}, Tb^{3+}, Dy^{3+}, Ho^{3+}, and Er^{3+} VIC's with 2-WLHS is positive and is linearly proportional to the de Gennes factor defined in Sec. III. The Curie-Weiss temperature of Ce^{3+}, Pr^{3+}, Nd^{3+}, and Sm^{3+} VIC's is negative and is proportional to $J(J+1)$. We determine the unit-cell stoichiometry of magnetic VIC's with 2-WLHS from the dc magnetic susceptibility and thermogravimetric measurements. We discuss the in-plane structure of rare-earth metal-ion VIC's with 2-WLHS.

II. EXPERIMENT

The samples described in this analysis were prepared from natural vermiculites obtained from Llano, Texas, which contain Mg^{2+} ions in the interlamellar space. These natural vermiculites were immersed in a 1N solution of rare-earth metal chlorides at 60 °C for 6 months. The Mg^{2+} ions can be replaced by rare-earth metal ions such as Ce^{3+}, Pr^{3+}, Nd^{3+}, Sm^{3+}, Eu^{3+}, Gd^{3+}, Tb^{3+}, Dy^{3+}, Ho^{3+}, and Er^{3+}, forming rare-earth metal-ion VIC's. The unit-cell stoichiometry of VIC's with 2-WLHS may be given in the form

$$(Si_{5.72}Al_{2.28})(Mg_{5.88}Al_{0.10}Fe_{u'}Ti_{0.02})O_{20}(OH)_4Z_u{}^{3+}(H_2O)v \ , \tag{1}$$

where Z^{3+} denotes a rare-earth metal ion as intercalant, u is the number of Z^{3+} ions, u' is the number of Fe ($u'=0.03$), and v is the number of water molecules per unit cell of $(a\times b)$. The total molar mass M of the unit-cell stoichiometry is given by $M=757.8+mu+18v$,[5] where m is the molar mass of Z^{3+} ion. The values of u and v for the rare-earth metal-ion VIC's were determined from the dc magnetic susceptiblity and thermogravimetric measurements.

The $(00L)$ x-ray diffraction of Mg^{2+}, Mn^{2+}, Co^{2+}, Ni^{2+}, Ce^{3+}, Pr^{3+}, Nd^{3+}, Sm^{3+}, Eu^{3+}, Gd^{3+}, Tb^{3+}, Dy^{3+}, Ho^{3+}, and Er^{3+} VIC's with 2-WLHS was measured at 300 K by using a Huber double circle diffractometer with a Mo $K\alpha$ x-ray radiation source (1.5 kW) and a highly oriented pyrolytic graphite monochromator. An entrance slit of 2×2 mm^2 was placed between the monochromator and sample. The x-ray beam diffracted by the sample was collimated by the exit slit of 0.7×0.7 mm^2 and detected by a Bicron photomultiplier tube. The dc magnetic susceptibility of the rare-earth metal-ion VIC's was measured by a Faraday electrobalance (Cahn RG) in the temperature range between 1.5 and 300 K. The magnetic field of $H=2$ kOe was applied to an arbitrary direction in the c plane of the samples. The details of the experimental procedure have been described in Refs. 3 and 5.

The dc magnetic susceptibility data were analyzed by a least-squares fit to the form

$$\chi_g=\frac{C_g}{T-\Theta}+\chi_g^0 \ , \tag{2}$$

where C_g is the gram Curie-Weiss constant, Θ is the Curie-Weiss temperature, and χ_g^0 is the temperature-independent susceptibility. The native magnetic ions (Fe) which exist in the octahedral sheet in the silicate layer also contribute to the paramagnetic susceptibility. The gram Curie-Weiss constant C_g can be described by

$$C_g=\frac{1}{8M}[uP_{\rm eff}^2(Z^{3+})+u'P_{\rm eff}^2({\rm Fe})] \ , \tag{3}$$

where $P_{\rm eff}(Z^{3+})$ and $P_{\rm eff}$(Fe) are the effective magnetic moments of Z^{3+} in the interlamellar space and the Fe ion in the octahedral sheet, respectively.[5] Since the Mg^{2+} ion has no magnetic moment, the Curie-Weiss susceptibility of the Mg^{2+} VIC with 2-WLHS arises from impurity Fe^{2+} or Fe^{3+} ions in the octahedral sites: $C_g=1.56\times10^{-4}$ emu K/g and $\Theta=-1.1$ K.[5] Since $M=921$, the value of $u'P_{\rm eff}^2$ (Fe) can be estimated as $u'P_{\rm eff}^2$ (Fe)$=1.15$ for $\mathbf{H}\|a$.

III. RESULTS

A. Structural properties of rare-earth metal-ion VIC's

The $(00L)$ x-ray diffraction of Mg^{2+}, Mn^{2+}, Co^{2+}, Ni^{2+}, Ce^{3+}, Pr^{3+}, Nd^{3+}, Sm^{3+}, Eu^{3+}, Gd^{3+}, Tb^{3+}, Dy^{3+}, Ho^{3+}, and Er^{3+} VIC's with 2-WLHS has been measured at 300 K. Figure 1 shows the $(00L)$ x-ray scattering intensity vs Q_c for (a) Ce^{3+} VIC with 2-WLHS and (b) Gd^{3+} VIC with 2-WLHS, where Q_c is the scattering wave vector. Very sharp Bragg peaks appear at Q_c

values given by $Q_c=(2\pi/d)L$, where d is the c-axis repeat distance and L is an integer. The full width at half maximum of each Bragg peak is almost independent of Bragg reflection index L, indicating the absence of Hendricks-Teller stage disorder. The c-axis repeat distance d of rare-earth metal-ion VIC's with 2-WLHS is determined from the method of least-squares fitting, and is listed in Table I. For comparison the values of d for Mg^{2+}, Mn^{2+}, Co^{2+}, and Ni^{2+} VIC's with 2-WLHS are also listed in Table I. Pastor, Rodriguez-Casellon, and Rodriguez Garcia[4] have reported the values of d for Ce^{3+}, Nd^{3+}, Gd^{3+}, Er^{3+}, and Mg^{2+} VIC's with 2-WLHS: $d=15.05$ Å for Ce^{3+}, 15.00 Å for Nd^{3+}, 14.82 Å for Gd^{3+}, 14.75 Å for Er^{3+}, and 14.40 Å for Mg^{2+}. These values of d are close to those listed in Table I. Figure 2 shows the relationship between d and the ionic radius R for transition-metal-ion VIC's with 2-WLHS and rare-earth metal-ion VIC's with 2-WLHS, where we use the values of R obtained by Shannon and Prewitt.[9] This result indicates that d is rougly proportional to the ionic radius. The value of d for rare-earth metal-ion VIC's ($\sim$14.9 Å) is larger than that for transition-metal-ion VIC's ($\sim$14.4 Å) because the ionic radius of rare-earth

TABLE I. The c-axis repeat distance d, the distance between intercalate and water layers c_1, the number of water molecules in the intercalate layer w, the values of $v-w$ with v listed in Table II, the Debye-Waller factor B introduced in Eq. (6).

	d (Å)	c_1 (Å)	w	$v-w$	B
Ce^{3+}	15.015±0.008	1.3	2.8	6.6	0
Pr^{3+}	14.964±0.046	1.6	3.2	6.8	30
Nd^{3+}	14.953±0.070	1.4	2.6	7.4	8
Sm^{3+}	15.031±0.241	1.4	2.9	7.5	0
Eu^{3+}	14.832±0.060	1.2	1.4	7.1	0
Gd^{3+}	14.860±0.020	1.8	3.2	8.7	42
Tb^{3+}	14.749±0.055	1.2	0	7.0	0
Dy^{3+}	14.914±0.011	1.7	4.0	7.3	27
Ho^{3+}	14.947±0.047	1.8	2.3	6.7	23
Er^{3+}	14.863±0.012	1.5	2.9	6.9	12
Mg^{2+}	14.434±0.005	1.22	0	6.25	15
Mn^{2+}	14.487±0.028	1.21	0	6.11	0
Co^{2+}	14.475±0.020	0.97	0	6.10	5
Ni^{2+}	14.369±0.004	0.92	0	6.45	13

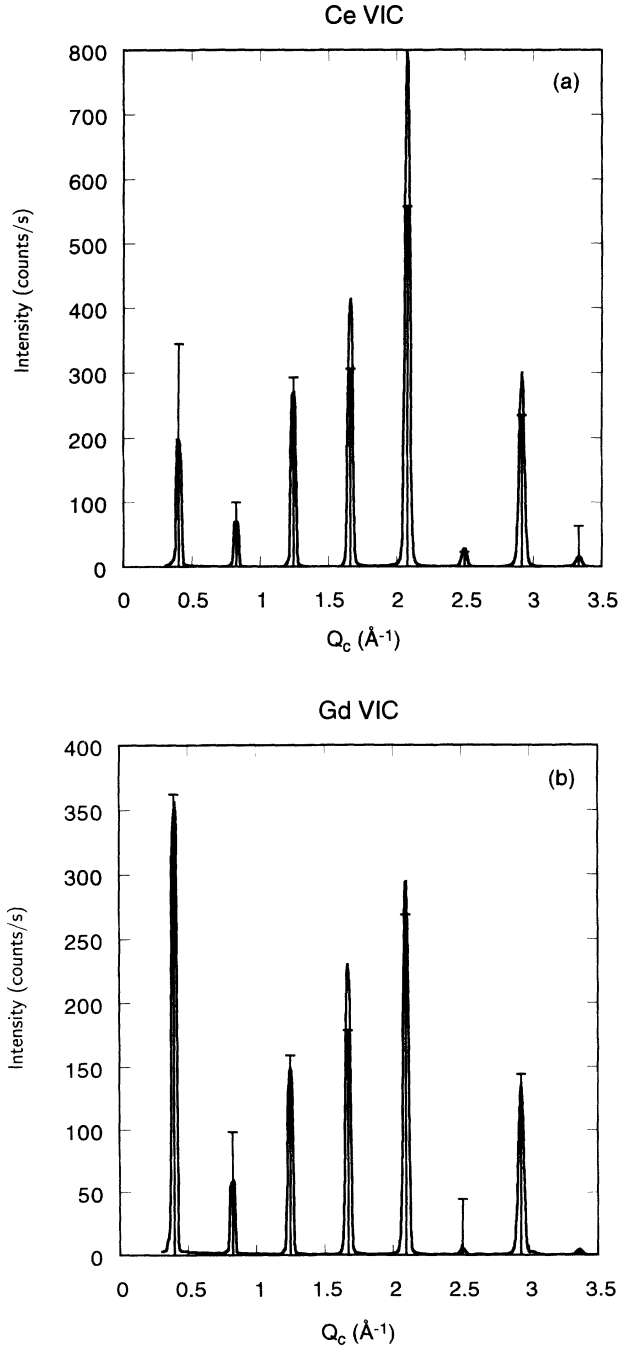

FIG. 1. (00L) x-ray-diffraction pattern for (a) Ce^{3+} and (b) Gd^{3+} VIC's with 2-WLHS at 300 K. The vertical lines are the calculated integrated intensities given by Eq. (6).

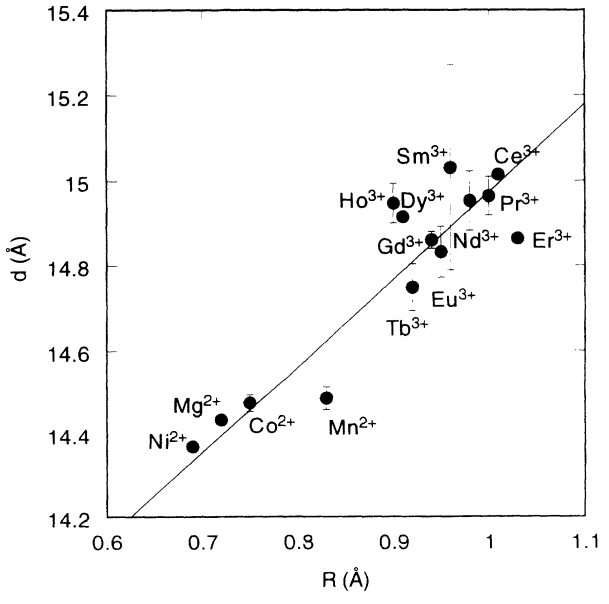

FIG. 2. c-axis repeat distance d (Å) vs ionic radius R (Å) for rare-earth metal-ion VIC's and transition-metal-ion VIC's with 2-WLHS. The solid line is a guide to the eye: $d=12.98+2R$.

metal ions is larger than that of transition-metal ions. In Fig. 2 the data of d vs R seem to fit well with the solid straight line expressed by $d=2R\pm(12.98\pm0.03)$, giving indirect evidence for the strong rigidity of the host silicate layers with respect to distortions involving displacements transverse to the layer plane.[10]

We notice that the $(00L)$ x-ray scattering intensity of rare-earth metal-ion Z^{3+} VIC's with 2-WLHS is very different from that of Mg^{2+} VIC with 2-WLHS.[1] The ratio of the integrated intensity at $L=1$ to that at $L=2$ is 74 for Mg^{2+} and 2–6 for rare-earth metal ions Z^{3+}. The integrated intensity at $L=7$ is almost the same as those at $L=6$ and 8 for Mg^{2+}, while the integrated intensity at the $L=7$ peak is much larger than those at $L=6$ and 8 for Z^{3+}. In order to explain this difference, here we propose the structure model for the c-axis stacking sequence of Z^{3+} VIC's with 2-WLHS in Fig. 3. In an $(a\times b)$ unit cell, w H_2O molecules lie in the same plane as u Z^{3+} rare-earth metal ions. This intercalate layer is sandwiched between two water layers having $\{(v-w)/2\}$ H_2O per unit cell. For Mg^{2+}, Mn^{2+}, Co^{2+}, and Ni^{2+} with 2-WLHS there is no water molecule in the intercalate layer: $w=0$. The structure factor of the Z^{3+} VIC with 2-WLHS is calculated as

$$S(Q_c)=uf_Z(Q_c)+w\{2f_H(Q_c)+f_O(Q_c)\}+(v-w)\{2f_H(Q_c)+f_O(Q_c)\}\times\cos(c_1Q_c)+(-)^{-L}S_{\text{silicate}}(Q_c)\,, \tag{4}$$

with

$$S_{\text{silicate}}(Q_c)=[5.88f_{Mg}(Q_c)+0.10f_{Al}(Q_c)+0.03f_{Fe}(Q_c)+0.02f_{Ti}(Q_c)+\{12f_H(Q_c)+4f_O(Q_c)\}\cos(1.06Q_c)+\{5.72f_{Si}(Q_c)+2.28f_{Al}(Q_c)\}\cos(2.73Q_c)+12f_O(Q_c)\cos(3.26Q_c)]\,, \tag{5}$$

where Q_c is measured in units of $Å^{-1}$, c_1 (Å) is the distance between intercalate layer and water layer, and $f_i(Q_c)$ is the atomic form factor for the i atom. Then the x-ray-scattering intensity along the Q_c direction is expressed by

$$I(00Q_c)=A|S(Q_c)|^2e^{-B(Q_c/4\pi)^2}\,, \tag{6}$$

where A is constant and the exponential factor with a constant B is a Debye-Waller factor.[11] A least-squares fit of the $(00L)$ x-ray integrated intensity vs Q_c to Eq. (6) yields values of w, c_1, A, and B for given d, u, and v, where u and v will be determined from both the dc magnetic susceptibility and thermogravimetric measurements later. The values of c_1, w, and B thus obtained are listed in Table I. The $(00L)$ x-ray intensity data of the Mg^{2+} VIC with 2-WLHS agree well with the calculated intensities derived from Eq. (6) with $u=0.93$: $w=0$, $d=14.434$ Å, $c_1=1.22$ Å, and $B=15$. We also find $w=0$ for Mn^{2+}, Co^{2+}, and Ni^{2+} VIC's with 2-WLHS, indicating that there is no water molecule in the same plane as cations for these VIC's. A least-squares fit of the $(00L)$ integrated intensity vs Q_c for the Ce^{3+} VIC with 2-WLHS to Eq. (6) yields $w=2.8$, $c_1=1.3$ Å, and $B=0$ for given values of u and v ($v=0.501$ and $v=9.43$). We find that the $(00L)$ x-ray intensity data for the rare-earth metal-ion VIC's with 2-WLHS agree well with the calculated intensities derived from Eq. (6) with d, w, c_1, $v-w$, and B listed in Table I. The values of w and c_1 depend on the cation species. The value of w is between 0 (Tb^{3+}) and 4.0 (Dy^{3+}), and the value of c_1 is between 1.2 Å (Eu^{3+}) and 1.8 Å (Gd^{3+}, Ho^{3+}).

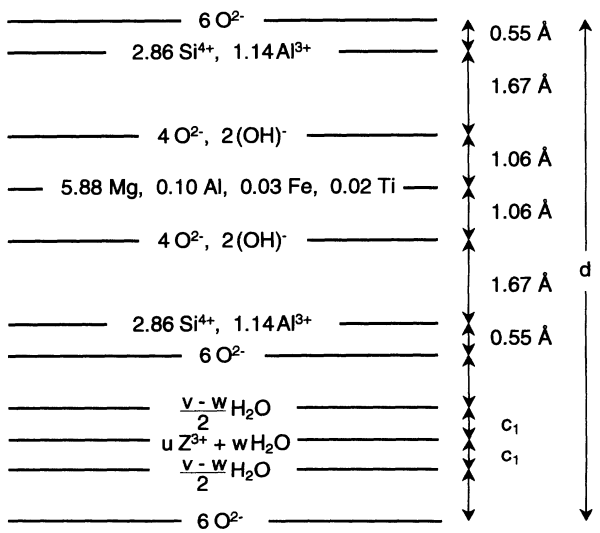

FIG. 3. Structural model of c-axis stacking sequence in rare-earth metal-ion VIC's with 2-WLHS, where d is the c-axis repeat distance.

B. Magnetic properties of rare-earth metal-ion VIC's

We have measured the dc magnetic susceptibility of Gd^{3+}, Tb^{3+}, Dy^{3+}, Ho^{3+}, and Er^{3+} VIC's with 2-WLHS in the temperature range between 1.5 and 300 K. Figure 4(a) shows the dc magnetic susceptibility of Gd^{3+}, Tb^{3+}, and Ho^{3+} VIC's with 2-WLHS as a function of temperature with the magnetic field along any direction perpendicular to the c axis ($H=2.0$ kOe). The dc magnetic susceptibility monotonically increases with decreasing tem-

perature, indicating no magnetic phase transition at temperatures down to 1.5 K. A least-squares fit of the data to Eq. (2) yields C_g and Θ as shown in Table II. The positive values of Θ for Gd^{3+}, Tb^{3+}, and Ho^{3+} VIC's with 2-WLHS indicate that the intraplanar exchange interaction is ferromagnetic. Figure 4(b) shows the reciprocal susceptibility $(\chi_g-\chi_g^0)^{-1}$ as a function of temperature for Gd^{3+}, Tb^{3+}, and Ho^{3+} VIC's with 2-WLHS. The reciprocal susceptibility of these compounds fits well with a straight line in the temperature range between 150 and 300 K, indicating that the magnetic susceptibility obeys a Curie-Weiss law. Suzuki *et al.*[5] have shown that the magnetic susceptibility of Dy^{3+} and Er^{3+} with 2-WLHS shows a Curie-Weiss behavior described by Eq. (2) with C_g and Θ listed in Table II. The positive values of Θ for Dy^{3+} and Er^{3+} with 2-WLHS also indicate that the intraplanar exchange interaction is ferromagnetic.

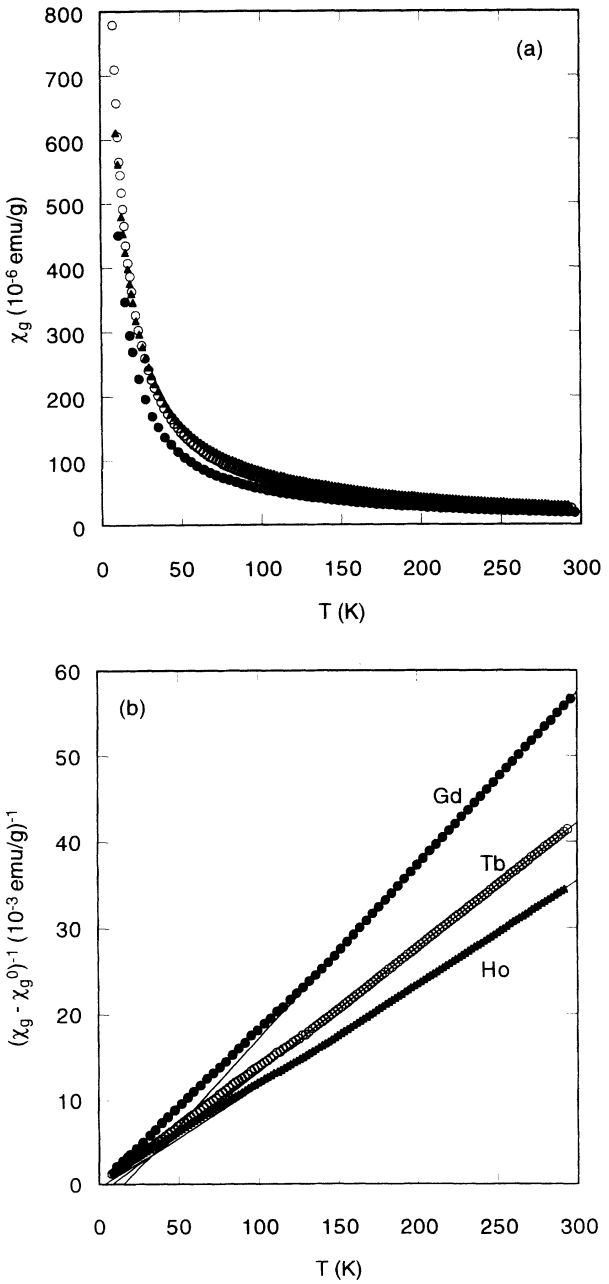

FIG. 4. (a) Temperature dependence of dc magnetic susceptibility for Gd^{3+} (●), Tb^{3+} (○), and Ho^{3+} (▲) VIC's with 2-WLHS. $H=2$ kOe and $H\perp c$. (b) Reciprocal susceptibility $(\chi_g-\chi_g^0)^{-1}$ as a function of temperature for Gd^{3+} (●), Tb^{3+} (○), and Ho^{3+} (▲) VIC's with 2-WLHS, where χ_g^0 is a temperature-independent susceptibility. The solid straight lines denote the Curie-Weiss law described by Eq. (2).

Next we compare the Gd^{3+} VIC with 2-WLHS and the Gd^{3+} VIC with 0-WLHS in order to analyze the effect the water layers have on the exchange interaction and the Curie-Weiss temperature. We have measured the dc magnetic susceptibility of the Gd^{3+} VIC with 0-WLHS in the temperature range between 1.5 and 300 K. No magnetic phase transition is observed for this compound. The dc magnetic susceptibility shows a Curie-Weiss behavior. A least squares-fit of the data to Eq. (2) yields $\Theta=-7.45\pm0.28$ K and $C_g=5.87\times10^{-3}$ emu K/g. In contrast, the Curie-Weiss temperature for the Gd^{3+} VIC with 2-WLHS is 15.31 ± 0.12 K. The sign of Θ for the Gd^{3+} VIC changes from positive to negative when the hydration state changes from 2-WLHS to 0-WLHS, indicating that the intraplanar exchange interaction changes from ferromagnetic to antiferromagnetic. Similar behaviors have been reported by Zhou *et al.*[8] for Mn^{2+}, Co^{2+}, Ni^{2+}, and Cu^{2+} VIC's with 0-WLHS, where the Curie-Weiss temperature of all the dehydrated compounds is negative. There are no water molecules in the interlamellar space of Gd^{3+} VIC's with 0-WLHS, as determined by Fig. 3 with $v=w=0$. In this case, the intercalate layer of Gd^{3+} ions is sandwiched just between upper and lower oxygen layers of the host silicate layer. The antiferromagnetic interaction between Gd^{3+} ions may be derived from a superexchange interaction via O^{2-}. The overlap of wave functions between the $2p$ orbit of O^{2-} and the $4f$ orbit of Gd^{3+} ions then leads to an antiferromagnetic path between NN Gd^{3+} ions. In this case the direct exchange interaction between NN Gd^{3+} ions must be smaller as compared to the superexchange interaction via the oxygen ions.

Next we study the dc magnetic susceptibility of the first three rare-earth ions Ce^{3+}, Pr^{3+}, and Nd^{3+} VIC's with 2-WLHS in the temperature range between 120 and 300 K. The measurements over the reduced temperature range were caused by technical difficulties but should not alter the overall conclusions. The dc magnetic susceptibility of these compounds obeys a Curie-Weiss law with a least-squares fit of the data yielding the values of C_g and Θ listed in Table II. Figure 5 shows the reciprocal susceptibility $(\chi_g-\chi_g^0)^{-1}$ as a function of temperature for Ce^{3+}, Pr^{3+}, and Nd^{3+} VIC's with 2-WLHS. We find that for Ce^{3+}, Pr^{3+}, and Nd^{3+} VIC's with 2-WLHS the Curie-Weiss temperature is negative, indicating that the intraplanar exchange interaction between NN magnetic ions is antiferromagnetic. This is in stark contrast to the previously studied heavy rare-earth metal ions in the 2-WLHS, which all showed a ferromagnetic exchange interaction. This will be discussed in more detail further below.

Next we study the dc magnetic susceptibility of the

TABLE II. Curie-Weiss temperature Θ, Curie-Weiss constant C_g, and the weight ratio δ of the 2-WLHS to the 0-WLHS for rare-earth metal-ion VIC's. The stoichiometric parameters u and v were determined from Eqs. (3) and (12). The data for Dy^{3+} and Er^{3+} VIC's with 2-WLHS were obtained by Suzuki *et al.* (Ref. 5).

	Θ (K)	C_g (10^{-3} emu K/g)	δ	u	v
Ce^{3+}	-10.82 ± 0.93	0.549 ± 0.002	1.205	0.501 ± 0.002	9.43
Pr^{3+}	-30.86 ± 0.49	1.01 ± 0.01	1.216	0.551 ± 0.002	10.02
Nd^{3+}	-39.84 ± 1.14	1.22 ± 0.01	1.211	0.685 ± 0.006	10.04
Sm^{3+}	-15.86 ± 1.65	0.189 ± 0.002	1.222	0.585 ± 0.025	10.43
Eu^{3+}			1.180	(0.62)	(8.52)
Gd^{3+}	15.31 ± 0.12	4.95 ± 0.01	1.249	0.657 ± 0.001	11.91
Tb^{3+}	8.25 ± 0.15	6.91 ± 0.01	1.149	0.557 ± 0.001	7.00
Dy^{3+}	10.6 ± 0.1	7.996	1.236	0.59	11.2
Ho^{3+}	3.34 ± 0.15	8.36 ± 0.01	1.189	0.596 ± 0.001	8.99
Er^{3+}	3.5 ± 0.1	6.78	1.204	0.60	9.72

two remaining rare-earth metal ions Sm^{3+} and Eu^{3+} which are situated between the light and heavy rare-earth metals. These two elements are expected to behave differently because of the known Van Vleck contribution to the susceptibility. Energy differences between successive J states are not large compared to k_BT at 300 K for Sm^{3+} and Eu^{3+}. Because of the influence of higher J states, the magnetic susceptibility of Sm^{3+} and Eu^{3+} has a different temperature dependence than the other rare-earth metal ions.[12] Figure 6(a) shows the temperature dependence of dc magnetic susceptibility for the Eu^{3+} VIC with 2-WLHS in the temperature range between 1.5 and 300 K. The dc magnetic susceptibility of the Eu^{3+} VIC with 2-WLHS shows a plateaulike behavior in the temperature range between 50 and 300 K. This temperature-independent term may correspond to the Van Vleck susceptibility of the Eu^{3+} ion. The Van Vleck susceptibility of Eu^{3+} is theoretically predicted by[13]

$$\chi_{VV}=\frac{N_A\mu_B^2}{k_B}\frac{8k_B/(E_1-E_0)+\exp[-(E_1-E_0)/k_BT]\{4.5/T+15k_B/(E_2-E_1)-8k_B/(E_1-E_0)\}}{1+3\exp[-(E_1-E_0)/k_BT]}, \tag{7}$$

where E_1-E_0 and E_2-E_1 correspond to the energy differences between the levels $^7F_1$ and $^7F_0$, and between $^7F_2$ and $^7F_1$, respectively. The values of E_1-E_0 and E_2-E_0 are estimated as 511 and 1471 K for $EuCl_3$,[14] and 510 and 1496 K for Eu_3S_4,[13] respectively. This Van Vleck susceptibility given by Eq. (7) is independent of temperature below 50 K. In Fig. 6(a) the dc magnetic susceptibility of the Eu^{3+} VIC with 2-WLHS rapidly increases with decreasing temperature below 50 K. The total susceptibility for the Eu^{3+} VIC with 2-WLHS is described by

$$\chi_g=Mu\chi_{VV}+\frac{C_g}{T-\Theta}+\chi_g^0 . \tag{8}$$

A least-squares fit of the data to Eq. (8) yields $C_g=1.16\times10^{-4}$ emu K/g and $\Theta=6\pm7$ K, where we use the values of $E_1-E_0=511$ K, $E_2-E_0=1471$ K, and $M=1005.38$ g. This assumes the number u as $u=0.62$, which will be discussed later. In Fig. 6(a) the solid line denotes the calculated susceptibility given by Eq. (8). The measured susceptibility agrees well with the calculated susceptibility above 30 K. The values of C_g and Θ for the Eu^{3+} VIC are in good agreement with those for the Mg^{2+} VIC with 2-WLHS: $C_g=1.56\times10^{-4}$ emu K/g

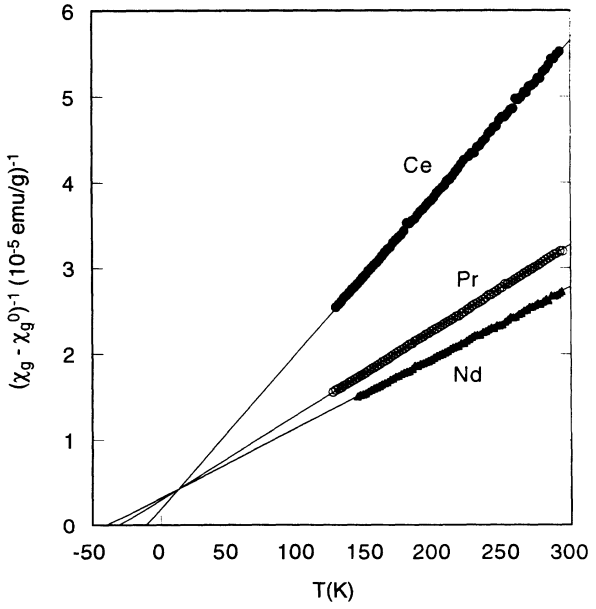

FIG. 5. Reciprocal susceptibility $(\chi_g-\chi_g^0)^{-1}$ as a function of temperature for Ce^{3+}, Pr^{3+}, and Nd^{3+} VIC's with 2-WLHS. The solid straight lines denote the Curie-Weiss law described by Eq. (2).

and $\Theta = -1.1$ K. This result indicates that the drastic change of the susceptibility at low temperatures arises from the Curie-Weiss behavior of Fe^{2+} or Fe^{3+} ions located in the octahedral sites of the host silicate. In Fig. 6(a) the Van Vleck and the Curie-Weiss contributions are denoted by a dash-dotted line and a dotted line, respectively. Note that the Van Vleck contribution is much larger than the Curie-Weiss contribution above 200 K.

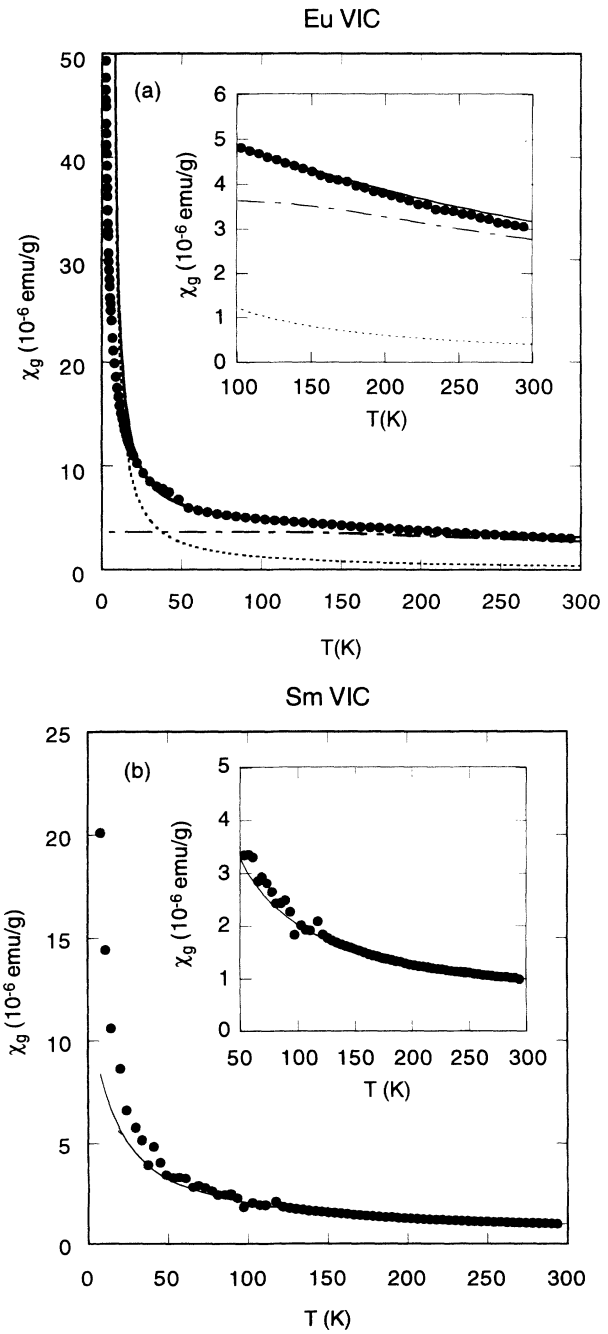

FIG. 6. Temperature dependence of dc magnetic susceptibility for (a) Eu^{3+} and (b) Sm^{3+} VIC's with 2-WLHS. $H=2$ kOe and $H \perp c$. In (a) Eu^{3+} VIC the Curie-Weiss and Van Vleck contributions are denoted by a dotted line and a dash-dotted line, respectively. The least-squares fitting curves are denoted by the straight lines in (a) and (b).

The Sm^{3+} VIC with 2-WLHS is also expected to show the Van Vleck susceptibility at high temperatures. The energy difference between $^6H_{7/2}$ and $^6H_{5/2}$ denoted by $E_{7/2}-E_{5/2}$ is about 1209 K and is much larger than k_BT below 300 K.[15] In this case Eq. (7) can be rewritten as

$$\chi_{VV}=\frac{C_M}{T-\Theta}+\frac{N_A\mu_B^2}{k_B}\left[\frac{\frac{20}{7}k_B}{E_{7/2}-E_{5/2}}\right], \tag{9}$$

where C_M is the molar Curie-Weiss constant defined by $C_M=(N_A\mu_B^2/3k_B)P_{\rm eff}^2(Sm^{3+})$. The effective magnetic moment of the Z^{3+} ion is theoretically calculated as

$$P_{\rm eff}(Z^{3+})g_J\sqrt{J(J+1)}\,, \tag{10}$$

where g_J is the Landé g factor and is given by[15,16]

$$g_J=\frac{3}{2}+\frac{S(S+1)-L(L+1)}{2J(J+1)}\,, \tag{11}$$

with total angular momentum J, spin angular momentum S, and orbital angular momentum L. The magnetic moment of rare-earth metal ions is directly bound to the presence of the $4f$ shell. The Hund rules give the values of S, L, and J for the most stable state. We notice that Eq. (9) is equivalent to the usual Curie-Weiss susceptibility. The second term is the contribution from the higher J states and is independent of temperature. Figure 6(b) shows the temperature dependence of dc magnetic susceptibility for the Sm^{3+} VIC with 2-WLHS. The susceptibility obeys the Curie-Weiss law in the temperature range between 150 and 300 K. A least squares-fit of the data to Eq. (2) yields C_g and Θ listed in Table II. Since the Sm^{3+} ion is one of the light rare-earth metal ions, it follows from Table II that Θ is negative for the light rare-earth metal ions (Ce^{3+}, Pr^{3+}, Nd^{3+}, and Sm^{3+}).

C. Unit-cell stoichiometry of rare-earth metal-ion VIC's

Now we determine the unit-cell stoichiometry of rare-earth metal-ion VIC's described by Eq. (1) from the dc magnetic susceptibility and thermogravimetric measurements. The gram Curie-Weiss constant C_g for the VIC's with rare-earth metal-ion Z^{3+} as intercalant can be described by Eq. (3) with $u'P_{\rm eff}^2(Fe)=1.15$. The values of C_g for Z^{3+} VIC's with 2-WLHS except for Eu^{3+} are listed in Table II. The effective magnetic moment $P_{\rm eff}(Z^{3+})$ is assumed to be given by Eq. (10). Furthermore we have determined the weight ratio δ of sample Z^{3+} VIC's with 2-WLHS to that with 0-WLHS from the thermogravimetric measurements. The ratio δ for each VIC thus obtained is listed in Table II. This ratio δ is expressed by

$$\delta=\frac{757.8+mu+18v}{757.8+mu}\,. \tag{12}$$

Once the values of C_g and δ are experimentally determined, the values of u and v for each Z^{3+} VIC can be estimated as listed in Table II from Eqs. (3) and (12). The value of u is expected from the theoretical model to be equal to $u=(\frac{2}{3})\times 0.93=0.62$ for complete exchange of the Mg^{2+} ions by Z^{3+} ions

$$M_g^{2+}\rightarrow\tfrac{2}{3}Z^{3+}\,. \tag{13}$$

It is difficult to determine the stoichiometry of the Eu^{3+} VIC from the above method because the susceptibility of the Eu^{3+} VIC with 2-WLHS does not obey the Curie-Weiss law at high temperatures. For convenience here we assume that the complete exchange of Mg^{2+} with Eu^{3+} occurs for the Eu^{3+} VIC ($u=0.62$). In Ce^{3+}, Pr^{3+}, Sm^{3+}, Tb^{3+}, Dy^{3+}, and Ho^{3+} VIC's with 2-WLHS u is smaller than 0.62, indicating a possibility of incomplete ion exchange. Hydrolysis may occur for u larger than 0.62. Hydrolysis gives rise to the dissociation of water coordinated to Z^{3+} ions, leading to

$$[Z^{3+}(H_2O)_n]_x^{3+}[Z^{3+}(H_2O)_{n-1}(OH)^{1-}]_y^{2+} , \quad (14)$$

in the interlamellar space, where $u=x+y$, and charge neutrality requires that $3x+2y=0.93\times 2=1.86$: $x=1.86-2u$, and $y=3u-1.86$. This assumes that Z^{3+} ions are not further hydrolyzed to, for example, $[Z^{3+}(H_2O)_{n-2}(OH)_2^{1-}]^{1+}$. In Nd^{3+} and Gd^{3+} VIC's with 2-WLHS, u is larger than 0.62, indicating a possibility of hydrolysis: $x=0.49$ and $y=0.17$ for Nd^{3+}, and $x=0.55$ and $y=0.11$ for Gd^{3+}.

D. In-plane structure model

Figure 7 shows the in-plane structure model of magnetic VIC's with $u=\frac{2}{3}$.[5] The in-plane structure of magnetic ions forms a distorted triangular lattice with the unit cell of $(3a\times b)$, where all magnetic ions sit over the sites belonging to one of the m_1, m_2, and m_3 sites. Note that all magnetic ions sit over the m_1 sites in Fig. 7. The m_1 and m_2 sites are located between those triangular groups of surface oxygens forming the bases of the SiO_4 and AlO_4 tetrahedron. The large magnetic ions tend to sit over the ditrigonal cavity (m_3 site). For the Gd^{3+} VIC the value of u is very close to $u=\frac{2}{3}$ and the ionic radius R is relatively large ($R=0.94$ Å), which may suggest that the in-plane structure is the $u=\frac{2}{3}$ type $(3a\times b)$ commensurate structure where Gd^{3+} ions sit over the m_3 sites. The distance between NN Gd^{3+} ions is 9.24 Å.

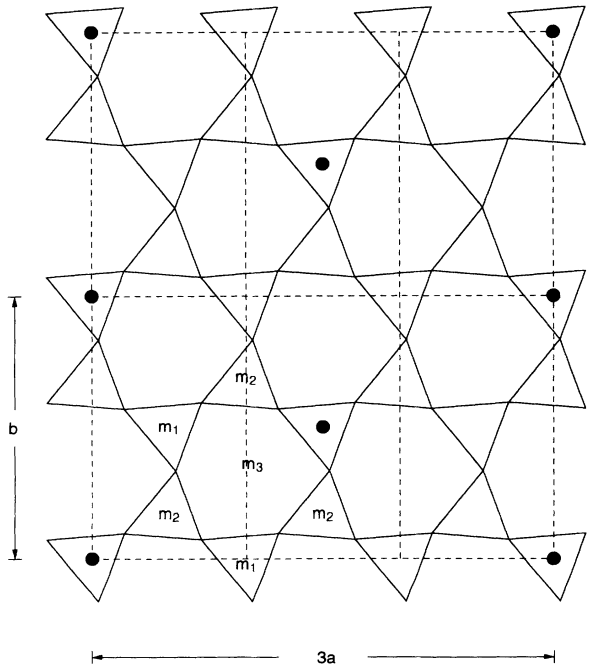

FIG. 7. In-plane models of rare-earth metal-ion VIC's with $u=\frac{2}{3}$, where u is the number of magnetic ions per unit cell $(a\times b)$. m_1, m_2: tetrahedral bases. m_3: ditrigonal cavities.

We now discuss the number of water molecules per unit cell in the interlamellar space between the host silicate layers. As shown in Fig. 3 there are $(v-w)$ H_2O in the upper and lower water layers and w H_2O in the same layer as the rare-earth metal ions for the rare-earth metal-ion VIC's with 2-WLHS. It is found from Table I and Table II that $v-w=6.6-8.7$ and $w=0-4.0$ for the rare-earth metal-ion VIC's with 2-WLHS, and that $v-w=6.11-6.45$ and $w=0$ for the transition-metal-ion VIC's with 2-WLHS. The values of $(v-w)$ for the rare-earth metal-ion VIC's with 2-WLHS is on the same order as that for the transition-metal-ion VIC's with 2-WLHS: typically $v-w=6.6$ for the Ce^{3+} VIC with 2-WLHS and $v=6.45$ for the Ni^{2+} VIC with 2-WLHS.

IV. DISCUSSION

We discuss here the magnetic properties of rare-earth metal-ion VIC's with 2-WLHS. We find that Θ is positive for heavy rare-earth metal ions (Gd^{3+}, Tb^{3+}, Dy^{3+}, Ho^{3+}, and Er^{3+}) and negative for light rare-earth metal ions (Ce^{3+}, Pr^{3+}, Nd^{3+}, and Sm^{3+}). In Fig. 8(a) we make a plot of Θ for heavy rare-earth metal ions as a function of the de Gennes factor defined by[15,16]

$$\xi=(g_J-1)^2J(J+1) . \quad (15)$$

In general the spin $\mathbf{S}$ is described by $\mathbf{S}=\mathbf{S}^{\parallel}+\mathbf{S}^{\perp}$, where $\mathbf{S}^{\parallel}=(g_J-1)\mathbf{J}$ and $\mathbf{S}^{\perp}$ are the components of $\mathbf{S}$ parallel and perpendicular to $\mathbf{J}$, respectively. In Fig. 8(a) we find that all the data of Θ fit well with a straight line described by a relation $\Theta=(0.93\pm 0.05)\xi$. Since $\mathbf{S}^{\parallel}\cdot\mathbf{S}^{\parallel}=(g_J-1)^2J(J+1)$, this linear relation suggests that the exchange interaction energy between heavy rare-earth metal ions located at the positions denoted by $\mathbf{R}_i$ and $\mathbf{R}_j$ may be described by

$$E(i,j)=-2J_{\text{exch}}\mathbf{S}_i^{\parallel}\cdot\mathbf{S}_j^{\parallel} , \quad (16)$$

where J_{exch} is the intraplanar exchange interaction between NN heavy rare-earth metal ions. We note that this exchange energy does not depend on the orbital angular momentum. The Curie-Weiss temperature Θ may be written as

$$\Theta=\frac{2zJ_{\text{exch}}}{3k_B}\xi , \quad (17)$$

where z is the number of NN ions. Since z is assumed to be equal to 6, the intraplanar exchange interaction J_{exch} can be estimated as $J_{\text{exch}}/k_B=0.233$ K, which is smaller than that for the Ni^{2+} VIC with 2-WLHS ($J_{\text{exch}}/k_B=0.88$ K).[5] Note that the dipole-dipole interaction between pair spins may be described by

$$H_d = \frac{g^2\mu_B^2}{r^3}(\mathbf{S}_1\cdot\mathbf{S}_2 - \mathbf{S}_1^z\mathbf{S}_2^z) , \tag{18}$$

where r is the positional vector connecting pair spins and is assumed to be parallel to the z axis, and the g factor is assumed to be isotropic. The dipole-dipole interaction ($g^2\mu_B^2/k_Br^3$) is estimated as 3.2 mK if $g=2$ and $r=9.24$ Å. Therefore the dipole-dipole interaction is negligibly small compared with the intraplanar exchange interaction. The intraplanar exchange interaction may arise from a long-range exchange interaction of the Ruderman-Kittel-Kasuya-Yosida (RKKY) type via polarization of conduction electrons.[15,16] The water molecules lying in the same plane as cations may also act as a media for the indirect intraplanar exchange interaction.

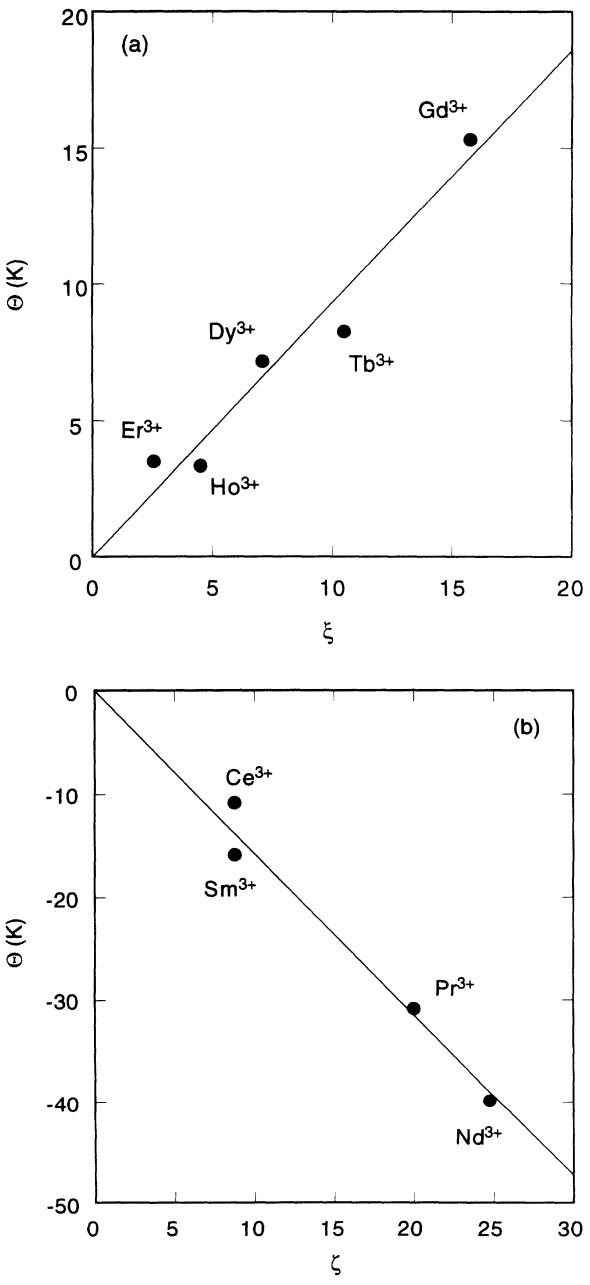

FIG. 8. (a) Θ vs ξ for Gd^{3+}, Tb^{3+}, Dy^{3+}, Ho^{3+}, and Er^{3+} VIC's with 2-WLHS, where $\xi=(g_J-1)^2J(J+1)$. The solid line is described by $\Theta=0.93\xi$. (b) Θ vs ζ for Ce^{3+}, Pr^{3+}, Nd^{3+}, and Sm^{3+} VIC's with 2-WLHS, where $\zeta=J(J+1)$. The solid line is described by $\Theta=-1.58\zeta$.

In Fig. 8(b) we make a plot of Θ for light rare-earth metal ions (Ce^{3+}, Pr^{3+}, Nd^{3+}, and Sm^{3+}) as a function of ζ [$=J(J+1)$] instead of the de Gennes factor. We find that all the data of Θ fit well with a straight line described by a relation $\Theta=(-1.58\pm0.06)\zeta$. Since $\mathbf{J}^2=J(J+1)$, this relation suggests that the exchange interaction energy between light rare-earth metal ions located at the positions denoted by $\mathbf{R}_i$ and $\mathbf{R}_j$ may be described by

$$E'(i,j) = -2J'_{\text{exch}}\mathbf{J}_i\cdot\mathbf{J}_j , \tag{19}$$

where $\mathbf{J}_i$ is the total angular momentum vector at $\mathbf{R}_i$, and J'_{exch} is the intraplanar exchange interaction between NN light rare-earth metal ions. This exchange energy depends only on the total angular momentum. The Curie-Weiss temperature Θ may be written as

$$\Theta = \frac{2zJ'_{\text{exch}}}{3k_B}\zeta . \tag{20}$$

Then the intraplanar exchange interaction J'_{exch} is antiferromagnetic and can be estimated as $J'_{\text{exch}}/k_B=-0.395$ K, which is in contrast with the ferromagnetic exchange interaction ($J'_{\text{exch}}/k_B=0.233$ K) for the heavy rare-earth metal ions. Note that the magnetic moment of each ion is described by $-\mu_B\mathbf{J}$ for the light rare-earth metal ions, and by $-(g_J-1)\mu_B\mathbf{J}$ for the heavy rare-earth metal ions. Such a difference may be caused by the degree of balance between the spin-orbit coupling and the crystal-field effect. For the light rare-earth metal ions the spin-orbit coupling is assumed to be dominant compared to the crystal field. Further study will be needed to understand (i) the origin of a long-range intraplanar exchange interaction which extends over a distance 9.24 Å, and (ii) the mechanism determining whether the intraplanar exchange interaction is ferromagnetic or antiferromagnetic.

V. CONCLUSIONS

The rare-earth metal VIC's with 2-WLHS may provide the model system for studying two-dimensional (2D) magnetism of rare-earth metal ions. Incomplete exchange from Mg^{2+} to Z^{3+} occurs for Ce^{3+}, Pr^{3+}, Sm^{3+}, Tb^{3+}, Dy^{3+}, Ho^{3+}, and Er^{3+} ($u<0.62$). Hydrolysis occurs in the interlamellar space for Nd^{3+} and Gd^{3+} ($u>0.62$). Because u is close to $\frac{2}{3}$, the in-plane structure of rare-earth metal ions may form a $(3a\times b)$ commensurate structure having two ions in this unit cell, where the NN distance between ions is about 9.24 Å. The Curie-Weiss temperature Θ of light rare-earth metal-ion VIC's is described as $\Theta=-1.58J(J+1)$, indicating that the crystal field is much weaker than the spin-orbit coupling. The Curie-Weiss temperature Θ of heavy rare-earth metal-ion VIC's is related to the de Gennes factor ξ as

$\Theta = 0.93\xi$. We interpret the intraplanar exchange interaction as arising from the long-range RKKY mechanism. The intraplanar exchange interaction of the Gd^{3+} VIC changes from ferromagnetic to antiferromagnetic as the hydration state changes from the 2-WLHS to 0-WLHS. Our interpretation is that the antiferromagnetic interaction is due to a superexchange interaction via O^{2-}. Further study will include the effect of hydration state on the magnetic properties of rare-earth metal-ion VIC's.

ACKNOWLEDGMENTS

We would like to thank M. Stanley Whittingham for useful discussion on the stoichiometry of vermiculite intercalation compounds. We are grateful to Floyd Khemai, Mitchell Johnson, and William Brinkman for their help on the x-ray-scattering and dc magnetic susceptibility measurements. This work was supported by NSF Grants No. DMR-8902351 and DMR-9201656.

[1]R. E. Grim, *Clay Mineralogy* (McGraw, New York, 1968); *Crystal Structures of Clay Minerals and their X-Ray Identification,* edited by G. W. Brindley and G. Brown (Mineralogical Society, London, 1980); H. van Olphen, *An Introduction to Clay Colloid Chemistry* (Wiley, New York, 1977).

[2]P. G. Slade, C. Dean, P. K. Schultz, and P. G. Self, Clays Clay Miner. **35**, 177 (1987).

[3]M. Suzuki, N. Wada, D. R. Hines, and M. S. Whittingham, Phys. Rev. B **36**, 2844 (1987).

[4]P. O. Pastor, E. Rodriguez-Casellon, and A. Rodriguez Garcia, Clays Clay Miner. **36**, 68 (1988).

[5]M. Suzuki, M. Yeh, C. R. Burr, M. S. Whittingham, K. Koga, and H. Nishihara, Phys. Rev. B **40**, 11 229 (1989).

[6]H. Nishihara, G. Kido, K. Koga, M. Suzuki, N. Wada, and Y. Nakamura, J. Magn. Magn. Mater. **90&91**, 81 (1990).

[7]N. Wada, M. Suzuki, D. R. Hines, K. Koga, and H. Nishihara, J. Mater. Sci. **2**, 864 (1987).

[8]P. Zhou, J. Amarasekera, S. A. Solin, S. D. Mahanti, and T. J. Pinnavaia, Phys. Rev. B **47**, 16 486 (1993).

[9]R. D. Shannon and C. T. Prewitt, Acta Crystallogr. B **25**, 925 (1969); **26**, 1046 (1970).

[10]B. R. York, S. A. Solin, N. Wada, R. Raythatha, I. D. Johnson, and T. J. Pinnavaia, Solid State Commun. **54**, 475 (1985).

[11]I. S. Suzuki and M. Suzuki, J. Phys. Condens. Matter **3**, 8825 (1991).

[12]R. M. White, *Quantum Theory of Magnetism* (Springer-Verlag, New York, 1983).

[13]P. Wachter, in *Valance Instabilities and Related Narrow-Band Phenomena,* edited by R. D. Parks (Plenum, New York, 1977), p. 337.

[14]J. A. Sommers and E. F. Westrum, Jr., J. Chem. Thermodyn. **9**, 1 (1977).

[15]*Magnetic Properties of Rare Earth Metals,* edited by R. J. Elliott (Plenum, New York, 1972).

[16]B. Coqblin, *The Electronic Structure of Rare-Earth Metals and Alloys: the Magnetic Heavy Rare-Earths* (Academic, New York, 1977).